Cx31 is assembled and trafficked to cell surface by ER-Golgi pathway and degraded by proteasomal or lysosomal pathways

Li Qiang HE*, Fang CAI, Yu LIU, Mu Jun LIU, Zhi Ping TAN, Qian PAN, Fai Yan FANG, De Sheng LIANG, Ling Qian WU, Zhi Gao LONG, He Ping DAI, Kun XIA**, Jia Hui XIA, Zhuo Hua ZHANG

National Laboratory of Medical Genetics, Central South University, Changsha 410078, China.

ABSTRACT

Gap junctions, consisting of connexins, allow the exchange of small molecules (<1 kD) between adjacent cells, thus providing a mechanism for synchronizing the responses of groups of cells to environmental stimuli. Connexin 31 is a member of the connexin family. Mutations on connexin 31 are associated with erythrokeratodermia variabilis, hearing impairment and peripheral neuropathy. However, the pathological mechanism for connexin 31 mutants in these diseases are still unknown. In this study, we analyzed the assembly, trafficking and metabolism of connexin 31 in HeLa cells stably expressing connexin 31. Calcein transfer assay showed that calcein transfer was inhibited when cells were treated with Brefeldin A or cytochalasin D, but not when treated with nocodazole or α-glycyrrhetinic acid, suggesting that Golgi apparatus and actin filaments, but not microtubules, are crucial to the trafficking and assembly of connexin 31, as well as the formation of gap junction intercellular communication by connexin 31. Additionally, α-glycyrrhetinic acid did not effectively inhibit gap junctional intercellular communication formed by connexin 31. Pulse-chase assay revealed that connexin 31 had a half-life of about 6 h. Moreover, Western blotting and fluorescent staining demonstrated that in HeLa cells stably expressing connexin 31, the amount of connexin 31 was significantly increased after these cells were treated with proteasomal or lysosomal inhibitors. These findings indicate that connexin 31 was rapidly renewed, and possibly degraded by both proteasomal and lysosomal pathways.

Keywords: connexin, Cx31, assembly, trafficking, metabolism.

INTRODUCTION

Gap junctions consisting of connexins, are able to mediate cell-cell communication via direct exchange of intercellular small molecules (< 1 kD). Generally, gap junctions are formed by homomeric or heteromeric hemichannels that are assembled by same or different kinds of connexins [1]. Willecke *et al* [2] screened mouse and human genomic databases and identified 19 connexin (*Cx*) genes in mouse genome and 20 *Cx* genes in human genome. Mutations on connexin have been identified in various hereditary diseases, including mutations of connexin 32 in Charcot Marie Tooth X-linked disease, connexin 26 and 30 in deafness and skin diseases, and connexin 46 and 50 in hereditary cataracts. Many mutated connexins have been reported to mistarget gap junctions and/or fail to oligomerize correctly into hemichannels. Genetic ablation approaches are helpful to map a connexin code and identify specific connexins required for cell growth and differentiation, as well as for basic intercellular communication [3].

Connexin 31 is an important member of the connexin family. Mutations in Cx31 would cause erythrokeratodermia variabilis (EKV), hearing impairment, and peripheral neuropathy, respectively [4–7]. However, the mechanism of Cx31 in the pathogenesis of these diseases remains unclear. Diestel *et al* reported that EKV-associated variant Cx31 (G12R) was expressed at comparable levels and localized at the plasma membranes, similar to wild type Cx31 (WT-Cx31); however, they displayed higher conduc-

*Current address: Institute of Medical Genetics, Medical School of Shanghai Jiao Tong University. 24#, lane 1400, West Beijing Road, Shanghai, China.

**Correspondence: Kun XIA
Tel: +86-731-4805357, Fax: +86-731-4478152,
Email: nlmglcy@xysm.net.

Abbreviations: AGA, α-glycyrrhetinic acid; ALLN, N-acetyl-leu-leu-norleu-al; BFA, Brefeldin A; CHX, cycloheximide; CLQ, chloroquine; CytoD, cytochalasin D; DiI, 1,1'-dioctadecyl-3,3,3',3'-tetramethylindocarbocyanine perchlorate; E-64, trans-epoxysaccinyl-L-leucylamide-(4-guanidino) butane; GJIC, gap junctional intercellular communication; Noc, nocodazole.

tance in dye couple studies than WT-Cx31 [8]. In addition, Di *et al* observed that four EKV-associated Cx31 variants (G12R, G12D, R42P, and C86S) showed defectiveness in trafficking to the plasma membrane, and the deafness/neuropathy associated variant (66delD) had a primarily cytoplasmic distribution, but some proteins were visualized at the plasma membrane in a few transfected cells [9]. However, the exact mechanism of how Cx31 is assembled and trafficked to cell membrane and then forms GJIC remains to be explored. Recently, Martin *et al* reported that multiple pathways were involved in the trafficking of Cx26, Cx32 and Cx43 and their assembly into gap junction intercellular communication channels [10]. Targeting of Cx32/CFP and Cx43/GFP to gap junctions and gap junctional communication was inhibited in cells treated with Brefeldin A (BFA), a drug that disassembles the Golgi apparatus. However, BFA had little effect on gap junctions formed by Cx26/GFP. Nocodazole (Noc), a microtubule disruptor, had little effect on the assembly of Cx43/GFP gap junctions, but perturbed the assembly of Cx26/GFP gap junctions. Co-expression of Cx26/YFP and Cx32/CFP in cells treated with BFA produced the assembly of Cx26/YFP gap junctions. Carsten and Karl found that microinjected anti-actin antibodies could reduce the intercellular communication of gap junction in cultured astrocytes, as cytochalasin D (cytoD) treatment did [11].

Unlike many other membrane proteins, connexins are relatively dynamic, for pulse-chase assays had demonstrated that most connexins have half-lives of 1–3 h in cultured cells [12–15]. Turnover, degradation, and remodeling of gap junctions may contribute substantially to the regulation of intercellular communication [16–18]. Previous studies have shown that proteins are degraded mainly by two pathways: lysosomal or proteasomal pathways. Notably, these two pathways have been implicated in the degradation of some connexins, e.g. Cx32 and Cx43.

This study investigated the function of Cx31 by using calcein transfer assay to clarify the pathway involved in the trafficking and assembly of Cx31 into GJIC, after cells expressing Cx31 were treated with BFA, CytoD, Noc, or α-glycyrrhetinic acid (AGA), respectively. We further studied the change of Cx31 with fluorescent microscopy and Western blotting to determine the Cx31 degradation pathway, after treating cells expressing Cx31 with protease inhibitors.

MATERIALS AND METHODS

Construct on chimeric Cx31 /EGFP and Cx31/myc

The *Cx31* gene sequence was PCR amplified from cDNA library. The primers used (Cx31-F/Cx31-R for *Cx31*/*EGFP*, Cx31-PCF/Cx31-PCR for *Cx31*/*myc*) were synthesized by Shanghai Bioasia (Tab. 1). The PCR conditions were: 5 min at 95°C; 30 cycles of 20 sec at 95°C, 30 sec at 62°C, and 45 sec at 72°C; 10 min at 72°C. Following the amplification, PCR products were cloned into pGEM-T vector (Promega). The recombinant plasmid Cx31/pGEM-T was digested by two restrictive enzymes (*Eco*R1 and *Sal*I for insertion into pEGFP-N1 or *Hind*III for pcDNA3.1/myc/His B^-), and the cutted off fragments were ligated into pEGFP-N1 vector (Clontech) or pcDNA3.1/myc/His B^- vector (Promega), respectively. The constructs were confirmed by sequencing..

Transfection of Cx31 constructs

HeLa cells, which are deficient in gap junctional intercellular communication, were obtained from ATCC and maintained in Dulbecco's modified Eagle's medium supplemented with 10% FBS (Gibco BRL), 100 U/ml penicillin, and 100 μg/ml streptomycin at 37°C in a moist atmosphere with 5% CO_2. Transfection was performed using Lipofectamine 2000 reagent (Invitrogen) according to the instructions of the manufacturer. Generally, a 1:2 (μg:μl) DNA: Lipofectamine 2000 was used for HeLa cells. Twenty-four hours after transfection, cells were harvested for Western blotting or immunoprecipitation, or fixed with cold methanol for fluorescence staining. To select stably expressing Cx31 or Cx31 mutant HeLa cell lines, cells were screened by adding G418 (800 μg/ml) at 24 h after transfection. The selective medium with G418 was renewed at 4 d intervals. For Cx31/EGFP, cell clones in which every cell exhibits green fluorescence were picked out for further culturing. For Cx31/myc, cell clones were removed and cultured for identification via Western blotting.

Time-lapse fluorescence microscopy

HeLa cells stably expressing *Cx31*/*EGFP* were plated in a culture dish with a coverslip, maintained in phenol red-free Hanks' medium containing Hanks' salt solution, 25 mM HEPES/DMEM (pH 7.4), 100 U/ml penicillin, 100 μg/ml streptomycin (all from Life Technologies), and 10% FBS. Before recording the motion of Cx31, Hoechst 33258 (1 μg/ml) for nucleus staining was added to the culture medium. During the process of recording, the temperature of the culture medium was maintained at 37°C. EGFP epifluorescence was

Tab. 1 Primer sequences for *Cx31*/*EGFP* and *Cx31*/*myc*.

Gene name	Forward primer	Reverse primer
Cx31/*EGFP*	CGGAATTC[a]TGGGCGCCATGGACTGGAAGACACTCCA	GCGTCGAC[b]TGGATGGGGGTCAGGTTGGG
Cx31/*myc*	CGGAATTC[a]GGCGCCATGGACTGGAAGACACTCCA	CCAAGCTT[c]GGGATGGGGGTCAGGTTGGG

a, restriction site sequence identified by *Eco*RI; b, restriction site sequence identified by *Sal*I; c: restriction site sequence identified by *Hind*III

recorded with a laser scanning confocal microscope (Bio-Rad).

Micoscopy and flow cytometry

HeLa cells stably expressing Cx31/myc were plated in 35 mm dishes the day before staining. Four hours before loading, HeLa cells were treated with BFA (5 μg/ml, Molecular Probes), cytoD (1 μg/ml, Sigma), Noc (20 μg/ml, Calbiochem), AGA (100 μg/ml, Sigma), N-acetyl-leu-leu-norleu-al (ALLN)(100 μg/ml, Sigma), or chloroquine (CLQ) (200 μg/ml, Sigma), respectively. For loading with calcein AM (C-3099; Molecular Probes, Eugene, OR) and 1, 1'-dioctadecyl-3, 3, 3', 3'-tetramethylindocarbocyanine perchlorate (DiI) (D-282; Molecular Probes), donor cells were washed once with 0.3 M glucose, and then incubated in 1 ml of staining solution (10 μM DiI, 5 μM calcein AM, 0.3 M glucose in distilled H_2O) at 37°C for 30 min. Following 5 min digestion in a 0.25% trypsin/0.02% EDTA solution, the donor cells were suspended in 1 ml 10%FBS/DMEM, centrifuged and then re-suspended in 1 ml 10% FBS /DMEM. The cells were added to a monolayer culture of unstained recipient cells at a ratio of 1:100 (donors: recipients). After 2 h of co-culturing, the cells were imaged using a laser scanning confocal microscope, and then trypsinized and suspended in PBS for further analysis by flow cytometry.

Suspended cells were diluted to a concentration of approximately 10^5 cells/ml and the fluorescence intensity was measured using a FACStar-Plus (Becton-Dickinson, Heidelberg, Germany) with a one-laser setup for OR an excitation wavelength of 488 nm. Emissions of calcein and DiI were determined after filtering with a 530/30 nm bandpass filter (FL1) and a 575/26 nm bandpass filter (FL2), respectively. Each sample was measured three times under a flow rate of 300–400 cells/s for 10,000–50,000 cells. Viable cells were selected by appropriately setting gates for forward light scattering at 488 nm with Cell Quest 3.1 software (Becton–Dickinson, Heidelberg, Germany).

Immunofluorescence staining

For staining the Golgi apparatus, HeLa cells were fixed with cold methanol for 15 min, given three 10 min washings with 0.1% Trition X-100/PBS, then stained with WGA (conjugated with Alexa fluor 594) for 15 min, and finally washed three times with PBS. To stain actin filaments and microtubule, and to detect the distribution of Cx31, HeLa cells were stained with mouse anti-β-actin monoclonal antibody (Sigma), mouse anti-β-tubulin monoclonal antibody (Sigma), and rabbit anti-Cx31 polyclonal antibody, respectively. Following several rinses, cells were incubated in the dark for 1 h at RT with CY2-conjugated goat anti-mouse IgG or CY3-conjugated goat anti-rabbit IgG (KPL). After rinsing with PBS, the coverslips were mounted onto glass slides and the cells were observed with a fluorescence microscope and imaged by a laser scanning confocal microscope (Bio-Rad).

Metabolic labeling analysis of Cx31

HeLa cells stably expressing *Cx31* at 90% confluence (in 35 mm dishes) were rinsed with methionine-deficient DMEM containing 10% dialyzed FBS and then labeled with methionine-deficient DMEM containing 10% dialyzed FBS and S^{35}-methionine (150 μCi/ml, EXPRE^{35}S^{35}S, NEG-072, Perkin Elmer) for 30 min. After rinsing with normal culture medium (DMEM supplemented with 10% FBS), cells were chased by normal culture medium supplemented with 450 μg/ml L-methionine for 0, 4, and 8 h. Cells were rinsed once with PBS and lyzed in RIPA on ice for 15 min. Insoluble cellular debris was cleared by centrifugation at 14,000 g for 10 min under a temperature of 4°C. After centrifugation, the supernatants were gathered for immunoprecipitation. Anti-Cx31 antibody (3 μg) and protein A agarose (KPL, 25 μl) were added to the lysates and incubated at 4°C overnight on a Mixer Genius. Following precipitation, protein-antibody-beads complexes were washed at least three times with RIPA. The proteins were separated on a 12% SDS-PAGE under denaturing conditions. Finally, the gel was dried in a vacuum pump and quantitated on a PhosphorImager (Molecular Dynamics) using IPLab Gel software.

Drug treatment

To analyze the Cx31 degradation pathway, HeLa cells stably expressing Cx31 were incubated with different drugs (20 μM ALLN (proteasomal inhibitor, Sigma), 200 μM leupeptin (Leu) (Sigma), 10 mM NH_4Cl, 100 μM CLQ (Sigma), 25 μM trans-epoxysaccinyl-L-leucylamide-(4-guanidino) butane (E-64) (Leu, NH_4Cl, CLQ, E-64 are all lysosomal inhibitors), and 20 μg/ml cycloheximide (CHX), or some combination of these drugs) for 6 h. HeLa cells were washed with PBS and harvested by scraping. The cells were then concentrated by centrifugation (1300 g, 5 min) and lysed with RIPA. Protein concentration was determined by a Bio-Rad Dc protein assay. Equal amounts of protein from each sample were separated with 10% SDS-PAGE. Following electrophoresis, the proteins were transferred to PVDF membrane. The PVDF membrane was then blocked overnight with 5% fat-lacking milk/3%BSA/PBS,.incubated with primary antibody (rabbit anti-Cx31 or anti-GFP polyclonal antibody 1:1000 Clontech) for 2 h and then with second antibody (HRP-conjugated goat anti-rabbit antibody 1:10000, Calbiochem) for 1 h. The PVDF membrane was washed three times with PBST and then detected by ECL (Amersham Biosciences). The same membrane was reused to detect β-tubulin expression as an internal control.

RESULTS

Dynamics of gap junctional plaques

A selection of pictures was taken from a typical series of micrographs recorded at 60 sec intervals for 60 min (Fig. 1). The movie generated from these pictures reveals that the multiple fluorescent plaques at the cell border between the two cells are highly dynamic (data not shown). Most molecules in these areas move around erratically and change shape constantly (see the region indicated by the rectangles in Fig. 1). The molecules often fuse with one another or separate into small parts (for example, see the region marked by the arrows in Fig. 1). Unlike the high mobility of the gap junctions at the cell surface, several large and strongly fluorescent cytoplasmic structures remained almost stationary, moving only a little throughout the observation period.

Pathway of trafficking and assembly of Cx31 into GJIC

BFA, CytoD, and Noc were found to be effective for disrupting the Golgi, actin filaments and the microtubules, respectively [10]. To find out the effects of drugs on the structure of HeLa cells, Golgi apparatus, actin filaments,

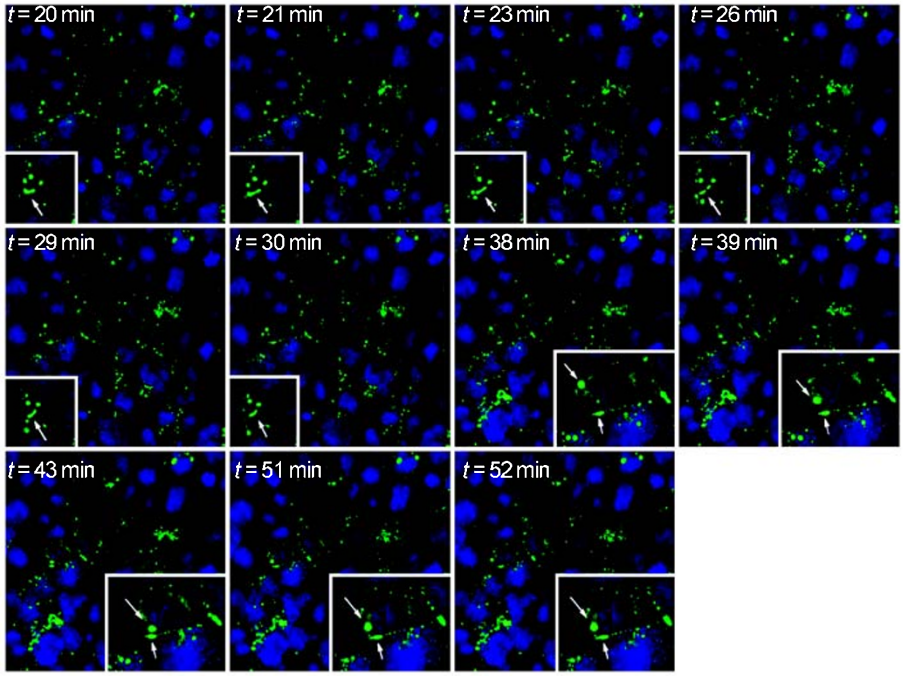

Fig. 1 Time series showing the dynamics of gap junction plaques within the plasma membrane of live HeLa cells. HeLa cells stably expressing *Cx31*/*EGFP* were imaged on an inverted confocal microscope over 60 min as described in the experimental procedures. The arrows denote a gap junction plaque that remains relatively dynamic throughout the experiment. Green, Cx31/EGFP; Blue, Hoechst 33258.

and microtubules were detected by WGA (confugated with Alexa Fluor 594), mouse anti-β-actin monoclonal antibody (Cy2 conjugated goat anti-mouse antibody as second antibody), and mouse anti-β-tubulin antibody (Cy2 conjugated goat anti-mouse antibodies as second antibody), respectively. Fig. 2 shows the results. Treatment of cells stably expressing Cx31/myc with BFA for 4 h caused disruption and redistribution of the Golgi apparatus to the perinuclear area (Fig. 2 A, B). Depolymerisation of the actin filaments was evident following treatment with cytoD (Fig. 2 C, D). After incubating the cells with Noc, β-tubulin staining indicated shattering of the microtubules (Fig. 2 E, F). Similar results were obtained after the HeLa cells stably expressing Cx31/GFP were treated with BFA, cytoD, or Noc. These observation results indicated the effectiveness of the drugs. These findings further confirmed what had been reported by Martin *et al* [10].

Figs. 3 and 4 show the percentages of calcein transfer among untreated cells and cells treated with different drugs for 4 h. After dispersion of the Golgi apparatus by BFA, or of the actin filaments by cytoD treatment, calcein transfer in cells expressing *Cx31*/*myc* was significantly reduced compared with non-treated cells, with transfer rates of 3.80% ($P < 0.001$) and 1.95% ($P < 0.001$), respectively. Conversely, Noc and AGA were not found to significantly affect the functionality of cells expressing *Cx31*/*myc*, with intercellular dye transfer in these cells being similar to untreated cells. These results suggested that efficient targeting of newly synthesized Cx31 to the plasma membrane and gap junction assembly required intact Golgi apparatus and actin filaments. During trafficking and assembly of Cx31, the effect of tubulin was not obvious. Although AGA is considered as a common inhibitor of GJIC [19], we observed little effect of Cx31 on GJIC .

To examine whether changes in intercellular communication induced by BFA or cytoD were reversible, HeLa cells treated with cytoD for 4 h were depleted of the drugs by thoroughly washing and then incubated in normal medium for 4 h. Fig. 3 (G, H) showed that calcein transfer could recur after a period of recovery, suggesting that GJIC were reversible after changes in intercellular communication induced by BFA or cytoD.

Additionally, the effect of drugs on intracellular redistribution of Cx31 was examined, with the results shown in Fig. 5. After treatment with BFA or cytoD, intracellular distribution of Cx31 was clearly changed compared to untreated HeLa cells. Most Cx31 was accumulated within the cytoplasm, and little was transferred to plasma membrane. In contrast, following incubation with Noc, most Cx31 was left in the plasma membrane, similar to non-treated

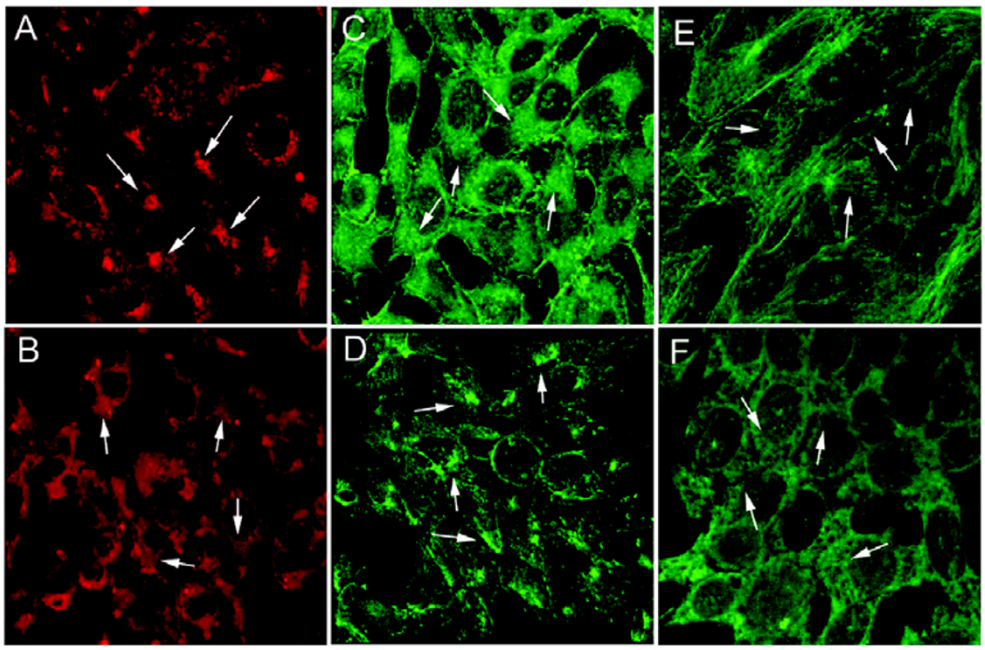

Fig. 2 Effect of BFA, Noc and CytoD on Golgi, microtubules and actin filaments **B**, **D**, and **F** were treated with 5 μg/ml BFA, 1 μg/ml cytoD, and 20 μg/ml Noc for 4 h, respectively. **A**, **C**, and **E** served as the control. Arrows show structural changes in the above figure following drug treatment. **A** and **B** were stained with WGA; **C** and **D** were stained with mouse anti-β-actin antibodies as primary antibodies and Cy2 conjugated goat anti-mouse antibodies as secondary antibodies and **E** and **F** were stained with mouse anti-β-tubulin antibodies as primary antibodies and Cy2 conjugated goat anti-mouse antibodies as secondary antibodies.

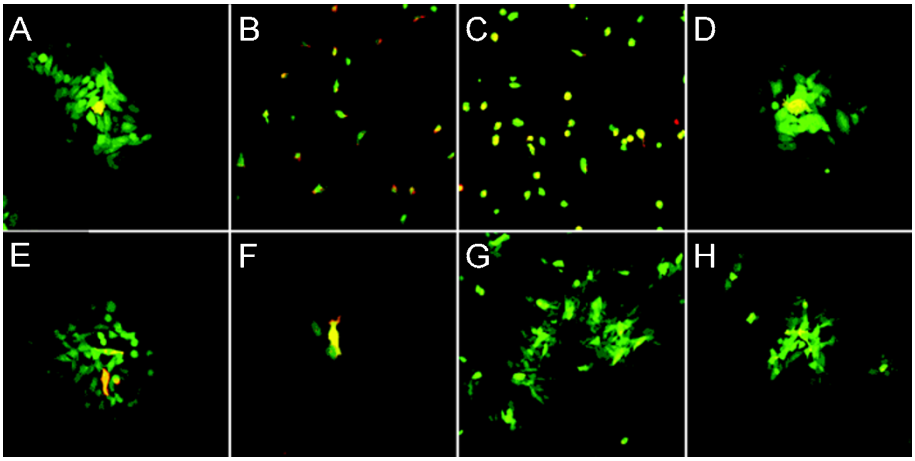

Fig. 3 Effect of different drugs on calcein transfer in HeLa cells expressing *Cx31/myc*. HeLa cells were not transfected with any plasmid or treated with any drugs to provide as control (**F**); HeLa cells stably expressing *Cx31/myc* were treated for 4 h with no drugs (**A**), BFA (**B**), cytoD (**C**), Noc (**D**), and AGA (**E**), respectively; HeLa cells stably expressing *Cx31/myc* were treated for 4 h with BFA (**G**), cytoD (**H**) and then washed and cultured with normal medium for 4 h. Red, DiI; Green, calcein; Yellow, a combination of DiI and calcein.

HeLa cells. This result is consistent with the FACS results of calcein transfer assay.

Degradation pathway of Cx31

Pulse-chase experiments were performed to investigate the rate of Cx31 turnover. The experimental results indicated that Cx31 had a half-life of approximately 6 h (Fig. 6 A). To explore the pathway of Cx31 degradation, HeLa cells stably expressing Cx31/myc were treated with different drugs for 4 h. These drugs included ALLN to inhibit proteasomal activity, CHX to inhibit protein synthesis, as well as CLQ, E64, NH_4Cl and Leu to inhibit lysosomal

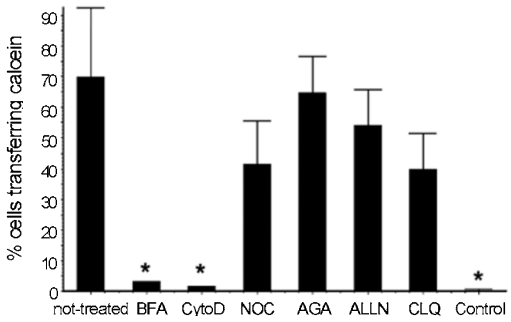

Fig. 4 Effect of inhibitors of the secretary pathway and cytoskeleton on intercellular transfer of calcein. HeLa cells that were not transfected with any plasmid or not treated with any drugs were used to provide a control (control); HeLa cells stably expressing *Cx31*/*myc* were treated for 4 h with no drugs (not-treated), BFA, cytoD, Noc, AGA, ALLN, and CLQ, respectively and then assayed for their ability to transfer calcein across gap junctions, as described in Materials and Methods. The results were expressed as the percentage of cells transferring dye to neighboring cells ± SD. Statistical significance was determined by Student *t*-test analysis. $P < 0.05$ was considered significant. *, $P < 0.001$.

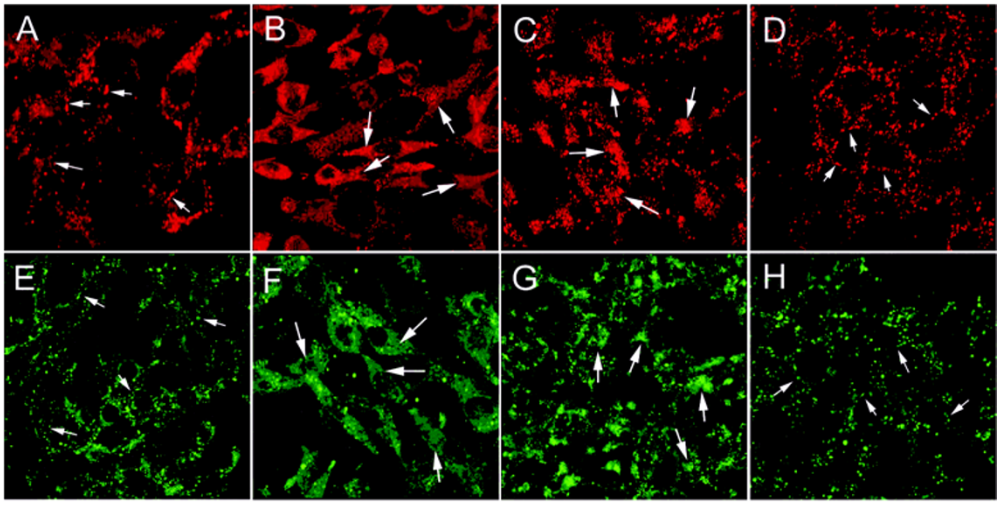

Fig. 5 Effect of different drugs on intracellular redistribution of Cx31. HeLa cells were treated for 4 h with no drug as a control (**A** and **E**), as well as with BFA (**B** and **F**), cytoD (**C** and **G**), Noc (**D** and **H**), respectively. For **A**, **B**, **C**, or **D**, HeLa cells stably expressing *Cx31*/*myc* were fixed for immunofluorescence staining with rabbit anti-Cx31 antibody as the primary antibody, and with Cy3 conjugated goat anti-rabbit antibody as the secondary antibody. For **E**, **F**, **G**, or **H**, HeLa cells stably expressing *Cx31*/*EGFP* were fixed for direct observation with a fluorescent microscope. Arrows show changes of gap junction plaques consisting of Cx31 following drug treatment.

activity. The Cx31 expressed in the whole cell lysate was then detected by Western blot. Fig. 6 shows the observation results. After treatment with CLQ, E-64, NH4Cl, or ALLN, the quantity of Cx31 clearly increased compared to the untreated control. Meanwhile, after treatment with CHX, the amount of Cx31 reduced obviously (Fig. 6B, C), showing that CHX effectively prevented from Cx31 synthesis. When Cx31 synthesis was inhibited, Cx31 degradation was clearly slowed by proteasomal or lysosomal inhibitors (Fig. 6C). Similar results were obtained for HeLa cells with stable expression of Cx31/EGFP (data not shown).

The changes in the amount and distribution of Cx31 in HeLa cells after drug treatment were detected using a confocal microscope. The observation indicated that Cx31 was mostly accumulated on the cellular membrane and in the cytoplasm after HeLa cells were treated with ALLN, CLQ, NH_4Cl, or E-64, while little expression was found in untreated HeLa cells. The quantity of Cx31 reduced in CHX treated HeLa cells compared to untreated ones (Fig. 7). These observations indicated that Cx31 degradation could be slowed down by proteasomal or lysosomal inhibitors.

Additionally, the influence of protease inhibitors on Cx31 function was examined via calcein transfer assay. The results showed that calcein transfer did not increase significantly for cells treated with ALLN or CLQ compared to non-treated cells (Fig. 4). This phenomenon suggested that the GJIC formed by Cx31 did not increase clearly, despite ALLN or CLQ inhibit Cx31 degradation.

In short, Cx31 degradation may occur via proteasomal or lysosomal pathways.

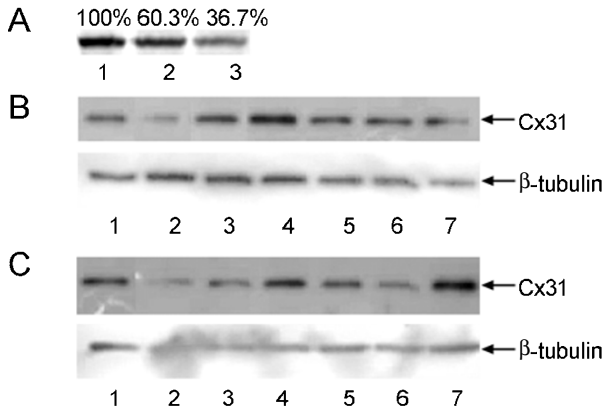

Fig. 6 Turnover rate and degradation pathway of Cx31. (**A**) HeLa cells stably expressing *Cx31*/*myc* were labelled with methionine-deficient DMEM containing 10% dialysed FBS and S^{35}-methionine for 30 min, then chased by normal culture medium supplemented with 450 μg/ml L-methionine for 0 h, 4 h, and 8 h, respectively. Cx31 in HeLa cells was gathered by immunoprecipitation and quantitated on a PhosphorImager using IPLab Gel software. (**B**) HeLa cells stably expressing *Cx31*/*myc* were treated for 4 h with no drugs as a control, and with CHX, ALLN, CLQ, E-64, Leu, and NH_4Cl, respectively. The Cx31 of whole cell lysates was then detected by Western blotting. (**C**) HeLa cells stably expressing *Cx31*/*myc* were treated for 4 h with no drugs, CHX, CHX + ALLN, CHX + CLQ, CHX + E-64, CHX + Leu, and CHX + NH_4Cl, respectively. Cx31 of whole cell lysates was then detected by Western blotting. In all the above experiments, β-tubulin was used as an internal Control. For each test, metabolic labeling and drug treatment were repeated for three times.

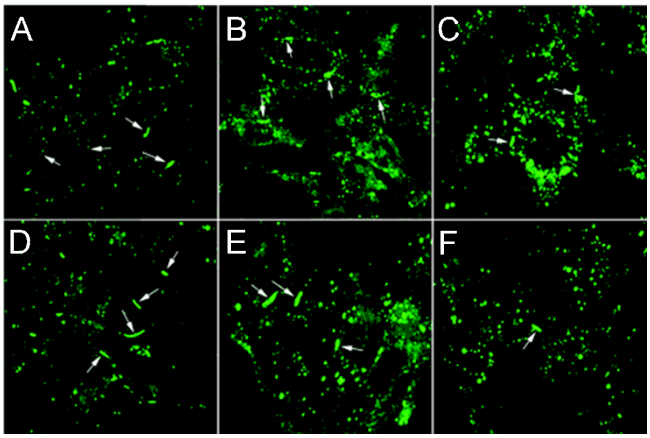

Fig. 7 Distribution of Cx31/EGFP in HeLa cells after drug treatment. HeLa cells stably expressing *Cx31*/*EGFP* were treated for 4 h with no drugs as a control (**A**), ALLN (**B**), CLQ (**C**), NH_4Cl (**D**), E-64 (**E**), and CHX (**F**), respectively. Then the distribution of Cx31 in HeLa cells was detected by fluorescent microscopy. Arrows show gap junction plaques consisting of Cx31.

DISCUSSION

The inherent fluorescent properties of GFP make it an excellent fusion partner for studying the trafficking, assembly, and secretion of both soluble and integral membrane proteins [20, 21]. When fused to GFP, most proteins retain their native targeting properties and traffic to the correct organelle [22, 23]. Several studies have examined the trafficking and functional characteristics of connexin-GFP fusion proteins [23, 24–28]. In this study, we generated a construct in which EGFP was fused to the carboxyl terminus of human Cx31. Notably, Cx31/EGFP was stably expressed in communication-deficient HeLa cells. The extreme similarity between the patterns of autofluorescence elicited by the fusion protein Cx31/EGFP and the indirect immunofluorescence of antibodies directed against GFP or connexin 31 (not shown) indicated that the detection of GFP fluorescence in living cells accurately reflects the distribution and trafficking of the chimeric polypeptides.

Time-lapse studies of living cells showed that gap junctional plaques formed by Cx31/EGFP are highly dynamic. Following delivery to the cell surface, Cx31/EGFP assembled into gap junction plaques that frequently coalesced within the plane of the cell membrane. The plaque regions are continuously moving at considerable speed, changing shape, and both fusing with one another and separating into smaller patches. Lateral coalescence and mobility of plaques have also been demonstrated for gap junctions formed by a connexin43-GFP chimera [24].

Connexins are known to be dynamic molecules with half-lives of 1–5 h [14, 29]. Pulse-chase assays performed in this study indicated that the half-life of Cx31 is approximately 6 h. The results of time-lapse and pulse-chase study indicate that gap junctions are constantly being formed and removed from the cell surface.

Vesicular trafficking from the endoplasmic reticulum via the Golgi apparatus is a common pathway for synthesized protein delivery, and is followed by most connexins, such as Cx43 and Cx32. However, Cx26 has an alternative route which does not involve trafficking through the Golgi apparatus, and which possibly involves post-translational insertion into either the endoplasmic reticulum or directly into the plasma membranes [3], indicating that multiple pathways may exist in cells for delivering connexins, particularly Cx26, to the cell membrane [10]. A complementary route to gap junctions was proposed owing to the inhibition of Cx32 and Cx43 trafficking, but not of Cx26 trafficking, to gap junctions after the disassembly of the Golgi apparatus induced by Brefeldin A (a fungal derived drug that dismantles the Golgi) or the temperature being lowered to 15°C in cell cultures expressing the

relevant connexins [10, 30]. Similar Cx26 intracellular trafficking independent of the Golgi was observed in hepatocytes prepared from livers of Cx32 knockout mice[31]. However, nocodazole, a drug that disassembles microtubules, blocked trafficking of Cx26 to gap junctions, but had little effect on trafficking of Cx32 and Cx43 [10].

To clarify the pathway for Cx31 trafficking and assembly, we detected the function of the gap junction by calcein transfer after the Golgi apparatus, microtubule or actin filaments were disrupted by BFA, Noc, or cytoD, respectively. The dye pre-loading method is simpler and more convenient than other methods. Furthermore, it can easily quantify the number of donor and acceptor cells for the calcein dye [19, 32]. The present results showed that calcein transfer was inhibited after the Golgi apparatus and actin filaments were disrupted by BFA and cytoD, respectively; however, calcein transfer was little affected when microtubules were disrupted by Noc. Therefore Cx31 may be delivered by vesicular trafficking from the endoplasmic reticulum via the Golgi apparatus. Intact actin filaments are likely to be important for targeting both connexins to gap junctions. Although microtubules are important in ER-Golgi trafficking, Noc had little effect on the onward transfer of Gogli to the gap junctions of Cx31. Similar effects have been reported in the trafficking of Cx32 and Cx43, not in that of Cx26 [10]. Like Cx26 and Cx32, Cx31 belongs to the β-subgroup of connexins, while Cx43 belongs to the α-subgroup. However, the assembly and traffic of Cx31 resembles that of Cx32 and Cx43, but not that of Cx26, suggesting that the trafficking pathway of connexins is not related to their phyologenetic positions.

Interestingly, disruption of the Golgi apparatus by BFA is reversible. The Golgi apparatus in animal cells is crucial in processing and sorting proteins, glycans and lipids destined for secretion or for other intracellular destinations. When the Golgi apparatus was dispersed by BFA, synthesis of Cx31 was not significantly damaged, but its trafficking was blocked. Cx31 could not be trafficked to cell membrane and accumulated in the cytoplasm. Consequently, the amount of Cx31 in the cytoplasm significantly increased after Cx31-expressing HeLa cells were treated with BFA (Fig. 5). The Golgi apparatus could be quickly formed once the effect of BFA was removed. Cx31 was then be trafficked to the cell membrane and formed gap junctional intercellular communication.

As a common inhibitor of GJIC [19], AGA was thought to indirectly block gap junctions by activating protein kinases, G-proteins or transport ATPases [33]. However, this study found that no discernable differences of calcein transfer in HeLa cells stably expressing Cx31 in the presence or absence of AGA. We thus concluded that AGA could not effectively inhibit the GJIC formed by Cx31. If so, some reports about the significance of gap junctional communication should be cautiously taken. For example, during preimplantation development several connexin proteins are expressed and assembled into gap junctions in the plasma membrane at compaction but the functional significance of connexin diversity remains controversial [34]. The opinion that function of connexin is not necessary for development of primplantation embryo is mainly based on the presumption that gap junction intercellular communication can be inhibited by AGA [35]. However, there are nine connexins (including Cx31) expressing during murine preimplantation development. The GJIC thus cannot be completely inhibited by AGA. Since no specific inhibitors are capable of blocking all potential channel types up to the present, it is difficult to know whether intercellular communication is dispensable for development of the preimplantation embryo [34]. Although gap junction channels are still widely considered to be large, non-specific pores connecting cells, the diversity of the connexin family led to more attention on the permeability characteristics of small molecules. Selective permeability to dye molecules differs among connexins, with variations occurring based on dye molecule size and charge[36]. Consequently, selecting suitable dye may be important for testing the function of special connexin. In this study, we select calcein to detect the function of GJIC formed by Cx31. There are remarkable differences of calcein transfer between HeLa cells stably expressing Cx31 and HeLa cells. We thus think that calcein is suitable for dye transfer assay to GJIC formed by Cx31.

To date, two proteolytic pathways have been implicated in connexin turnover in intact cells. The first pathway is the lysosome, demonstrated by electron microscopy localization studies to mediate the degradation of internalized gap junctional plaques in at least some cell lines [37]. The second pathway is the proteasome, the multi-catalytic protease complex that degrades most rapid turnover proteins in cytosol and nucleus and which is also involved in the degradation of proteins in the secretory pathway.

Pathways can be clarified by incubating cells with specific and selective inhibitors of the proteasome (peptide aldehydes such as ALLN or carboxybenzoyl-leucyl-leucyl-leucinal [MG132] or the fungal metabolite lactacystin) or the lysosome (lysosomotropic amines such as primaquine or chloroquine, weak bases such as ammonium chloride, or cathepsin inhibitors such as leupeptin or E-64) [38]. Using this approach, some connexins, for example, Cx43 and Cx32, were found to be degraded by both proteasomal and lysosomal pathways [13, 39]. This work studied pathways responsible for degrading Cx31 by incubating cells with specific and selective inhibitors of the proteasome or

the lysosome. Immunofluorescent staining assay and Western blotting study also confirmed that treatment HeLa cells with inhibitors of either pathway led to Cx31 accumulation, suggesting that both the lysosome and proteasome participate in Cx31 degradation. Thus degradation of connexins may commonly be involved in both the proteasomal and lysosomal pathways.

In summary, this study comprehensively analyzed the life cycle of Cx31. Similar to Cx32 and Cx43, but unlike Cx26, Cx31 is assembled and trafficked to cell membrane along the secretary pathway, which depends on an intact Golgi apparatus and actin filament, but not on microtubule. Similar to Cx32 and Cx43, Cx31 is degraded via proteasomal or lysosomal pathways.

ACKNOWLEDGEMENTS

This work was supported by "the National High Technology Research and Development Program of China, No. 2002BA711A07-03, 08, the Major State Basic Research Development Program of China, No. 2001CB510302 and 2004CB518800, and the National Natural Science Foundation of China, No. 30370737.

Received, March 1, 2005
Revised, May 26, 2005
Accepted, May 29, 2005

REFERENCES

1 Elfgang C, Eckert R, Lichtenberg-Frate H, et al. Specific permeability and selective formation of gap junction channels in connexin-transfected HeLa cells. J Cell Biol 1995; **129:**805-17.
2 Willecke K, Eiberger J, Degen J, et al. Structural and functional diversity of connexin genes in the mouse and human genome. Biol Chem 2002; **383:**725-37.
3 Evans WH, Martin PE. Gap junctions: structure and function. Mol Membr Biol 2002; **19:**121-36.
4 Liu XZ, Xia XJ, Xu LR, et al. Mutations in connexin31 underlie recessive as well as dominant non-syndromic hearing loss. Hum Mol Genet 2000; **9:**63-7.
5 Lopez-Bigas N, Olive M, Rabionet R, et al. Connexin 31 (GJB3) is expressed in the peripheral and auditory nerves and causes neuropathy and hearing impairment. Hum Mol Genet 2001; **10:** 947-52.
6 Richard G, Smith LE, Bailey RA, et al. Mutations in the human connexin gene GJB3 cause erythrokeratodermia variabilis. Nat Genet 1998; **20:**366-9.
7 Xia JH, Liu CY, Tang BS, et al. Mutations in the gene encoding gap junction protein beta-3 associated with autosomal dominant hearing impairment. Nat Genet 1998; **20:**370-3.
8 Diestel S, Richard G, Doring B, Traub O. Expression of a connexin31 mutation causing erythrokeratodermia variabilis is lethal for HeLa cells. Biochem Biophys Res Commun 2002; **296:**721-8.
9 Di WL, Monypenny J, Common JE, et al. Defective trafficking and cell death is characteristic of skin disease-associated connexin 31 mutations. Hum Mol Genet 2002; **11:**2005-14.
10 Martin PE, Blundell G, Ahmad S, Errington RJ, Evans WH. Multiple pathways in the trafficking and assembly of connexin 26, 32 and 43 into gap junction intercellular communication channels. J Cell Sci 2001; **114:**3845-55.
11 Theiss C, Meller K. Microinjected anti-actin antibodies decrease gap junctional intercellular commmunication in cultured astrocytes. Exp Cell Res 2002; **281:**197-204.
12 Darrow BJ, Laing JG, Lampe PD, Saffitz JE, Beyer EC. Expression of multiple connexins in cultured neonatal rat ventricular myocytes. Circ Res 1995; **76:**381-7.
13 Laing JG, Tadros PN, Westphale EM, Beyer EC. Degradation of connexin43 gap junctions involves both the proteasome and the lysosome. Exp Cell Res 1997; **236:**482-92.
14 Laird DW, Puranam KL, Revel JP. Turnover and phosphorylation dynamics of connexin43 gap junction protein in cultured cardiac myocytes. Biochem J 1991; **273:**67-72.
15 Musil LS, Beyer EC, Goodenough DA. Expression of the gap junction protein connexin43 in embryonic chick lens: molecular cloning, ultrastructural localization, and post-translational phosphorylation. J Membr Biol 1990; **116:**163-75.
16 Laird DW. The life cycle of a connexin: gap junction formation, removal, and degradation. J Bioenerg Biomembr 1996; **28:**311-8.
17 Risek B, Guthrie S, Kumar N, Gilula NB. Modulation of gap junction transcript and protein expression during pregnancy in the rat. J Cell Biol 1990; **110:**269-82.
18 Musil LS, Le AC, VanSlyke JK, Roberts LM. Regulation of connexin degradation as a mechanism to increase gap junction assembly and function. J Biol Chem 2000; **275:**25207-15.
19 Goldberg GS, Bechberger JF, Naus CC. A pre-loading method of evaluating gap junctional communication by fluorescent dye transfer. Biotechniques 1995; **18:**490-7.
20 Hanakam F, Albrecht R, Eckerskorn C, Matzner M, Gerisch G. Myristoylated and non-myristoylated forms of the pH sensor protein hisactophilin II: intracellular shuttling to plasma membrane and nucleus monitored in real time by a fusion with green fluorescent protein. Embo J 1996; **15:**2935-43.
21 Yano M, Kanazawa M, Terada K, et al. Visualization of mitochondrial protein import in cultured mammalian cells with green fluorescent protein and effects of overexpression of the human import receptor Tom20. J Biol Chem 1997; **272:**8459-65.
22 Naray-Fejes-Toth A, Fejes-Toth G. Subcellular localization of the type 2 11beta-hydroxysteroid dehydrogenase. A green fluorescent protein study. J Biol Chem 1996; **271:**15436-42.
23 Pedraza L, Fidler L, Staugaitis SM, Colman DR. The active transport of myelin basic protein into the nucleus suggests a regulatory role in myelination. Neuron 1997; **18:**579-89.
24 Jordan K, Solan JL, Dominguez M, et al. Trafficking, assembly, and function of a connexin43-green fluorescent protein chimera in live mammalian cells. Mol Biol Cell 1999; **10:**2033-50.
25 Lauf U, Giepmans BN, Lopez P, et al. Dynamic trafficking and delivery of connexons to the plasma membrane and accretion to gap junctions in living cells. Proc Natl Acad Sci 2002; **99:**10446-51.
26 Lopez P, Balicki D, Buehler LK, Falk MM, Chen SC. Distribution and dynamics of gap junction channels revealed in living cells. Cell Commun Adhes 2001; **8:**237-42.
27 Holm I, Mikhailov A, Jillson T, Rose B. Dynamics of gap junctions observed in living cells with connexin43-GFP chimeric protein. Eur J Cell Biol 1999; **78:**856-66.
28 Laird DW, Jordan K, Shao Q. Expression and imaging of connexin-

GFP chimeras in live mammalian cells. Methods Mol Biol 2001; **154:**135-42.
29 Traub O, Look J, Paul D, Willecke K. Cyclic adenosine monophosphate stimulates biosynthesis and phosphorylation of the 26 kD gap junction protein in cultured mouse hepatocytes. Eur J Cell Biol 1987; **43:**48-54.
30 George CH, Kendall JM, Evans WH. Intracellular trafficking pathways in the assembly of connexins into gap junctions. J Biol Chem 1999; **274:**8678-85.
31 Kojima T, Fort A, Tao M, Yamamoto M, Spray DC. Gap junction expression and cell proliferation in differentiating cultures of Cx43 KO mouse hepatocytes. Am J Physiol Gastrointest Liver Physiol 2001; **281:**G1004-13.
32 Czyz J, Irmer U, Schulz G, Mindermann A, Hulser DF. Gap-junctional coupling measured by flow cytometry. Exp Cell Res 2000; **255:**40-6.
33 Evans WH, Boitano S. Connexin mimetic peptides: specific inhibitors of gap-junctional intercellular communication. Biochem Soc Trans 2001; **29:**606-12.
34 Houghton FD. Role of gap junctions during early embryo development. Reproduction 2005; **129:**129-135.
35 Vance MM, Wiley LM. Gap junction intercellular communication mediates the competitive cell proliferation disadvantage of irradiated mouse preimplantation embryos in aggregation chimeras. Radiat Res 1999; **152:**544-51.
36 Nicholson BJ, Weber PA, Cao F, et al. The molecular basis of selective permeability of connexins is complex and includes both size and charge. Braz J Med Biol Res 2000; **33:**369-78.
37 Larsen WJ, Hai N. Origin and fate of cytoplasmic gap junctional vesicles in rabbit granulosa cells. Tissue Cell 1978; **10:**585-98.
38 Saffitz JE, Laing JG, Yamada KA. Connexin expression and turnover: implications for cardiac excitability. Circ Res 2000; **86:** 723-8.
39 VanSlyke JK, Deschenes SM, Musil LS. Intracellular transport, assembly, and degradation of wild-type and disease-linked mutant gap junction proteins. Mol Biol Cell 2000; **11:**1933-46.